Mem. Natl Inst. Polar Res., Spec. Issue, **43**, 1–12, 1986

SURFACE CONFIGURATION OF THE ANTARCTIC ICE SHEET IN THE SECTOR 30°E–80°E USING SEASAT ALTIMETRY DATA

Kazuo SHIBUYA[1], Yuko KAJIKAWA[2]* and Jiro SEGAWA[3]

[1]*National Institute of Polar Research, 9–10, Kaga 1-chome, Itabashi-ku, Tokyo 173*
[2]*Department of Physics, Tokai University, Kitakaname, Hiratsuka 259–12*
[3]*Ocean Research Institute, University of Tokyo, 15–1, Minamidai 1-chome, Nakano-ku, Tokyo 164*

Abstract: Using Interim Geophysical Data Record (IGDR) of SEASAT radar altimetry, a configuration map of the Antarctic ice sheet in the area bounded by 30° and 80°E and latitude 72°S is compiled. A total of 7480 footprint data of every second sampling (6.62 km apart) along 63 subsatellite groundtracks are obtained in the area. The area was divided into rectangles with side lengths of 0.1° in latitude and 0.4° in longitude, and the average elevation above sea level by SEASAT altimetry data within the rectangle is used for computer-aided contouring. Since the height error for 147 crossover points on the ice sheet was ±6.7 m in standard deviation, and height errors from slope-induced effect and other sources were 20 m, the contour interval of 100 m was chosen for an inland area higher than 500 m above sea level. The obtained configuration resembles the map published by the Scott Polar Research Institute (1983). A total of 157 ground survey data from triangulation survey, satellite Doppler positioning and previously published topographic map are used to estimate an overall accuracy of the obtained configuration map. The ground survey height is on an average 2.2 m lower than the SEASAT-derived elevation with a standard deviation of ±21.5 m, which may reflect the limited data quality of IGDR without retracking correction of the return-pulse waveform. Drawing orthogonals to the contours, ice drainage basins are determined and they are slightly different from the previous ones defined by the over-snow traverse surveys.

1. Introduction

With the accumulation of geodetic, barometric and airborne radar altimetry data in Antarctica, configuration mapping has been progressing. However, it took almost 20 years from the compilation of the SOVETSKAYA ANTARKTICHESKAYA EKSPEDITSIYA (1966) with 500 m contours to the map of Scott Polar Research Institute with 100 m contours edited by DREWRY (1983), which is hereafter referred to as SPRI map, and time change of the ice sheet morphology can hardly be traced. In contrast, the satellite altimetry can provide us with densely distributed data within a comparatively short observation period and has successfully been applied to the Antarctic and Greenland ice sheet mapping. For example, BROOKS *et al.* (1978) obtained the configuration of South Greenland using GEOS-3 data. ZWALLY *et al.* (1983) contoured the East Antarctic ice sheet between 70° and 160°E at 100 m intervals using SEASAT-1 radar altimetry data.

* Present address: Japan Process Development Co., Ltd., 23–16, Ofuna 1-chome, Kamakura 247.

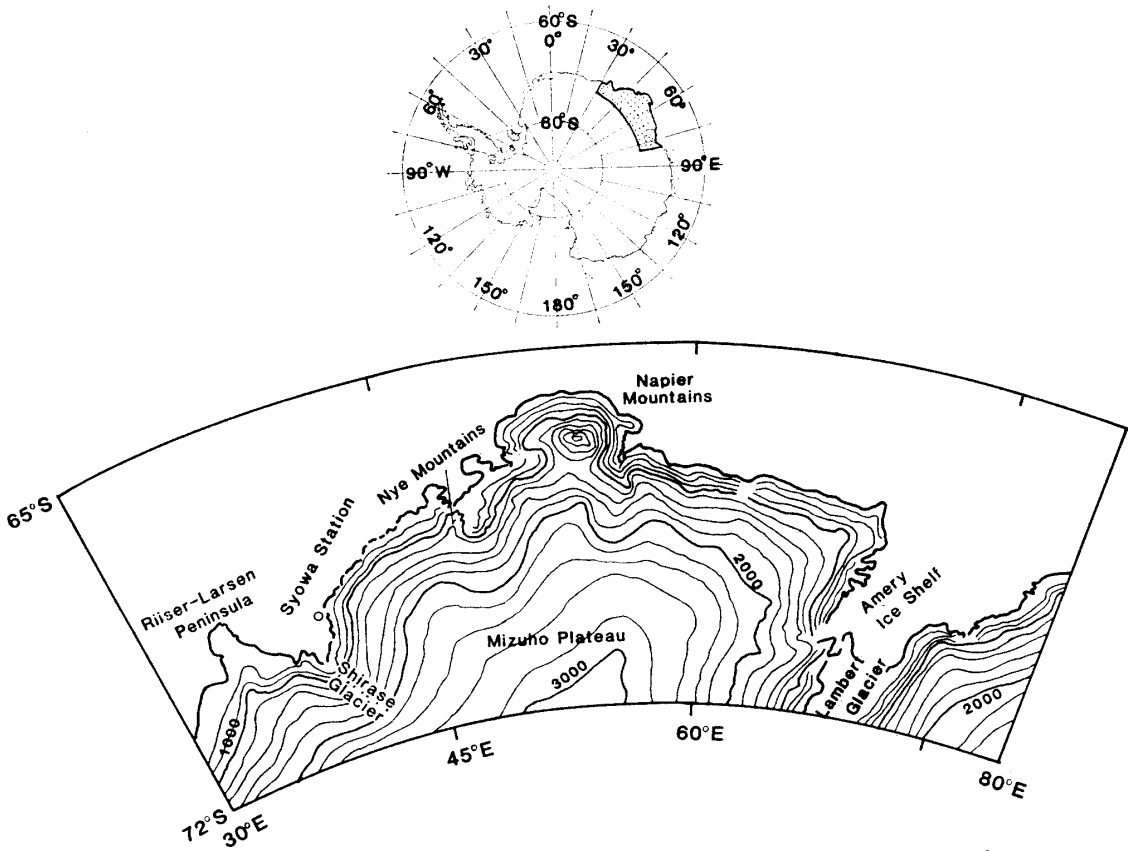

Fig. 1. The selected area for topographic mapping by the SEASAT altimetry data. The lower sector indicates 200 m contouring compiled from DREWRY *(1983).*

In this report, we also used SEASAT-1 radar altimetry data for contouring the Antarctic ice sheet between 30° and 80°E (Fig. 1). After examining orbit determination errors, the elevation values interpolated from the SEASAT configuration map (SEASAT elevations) are compared with the ground survey elevations obtained by the Japanese Antarctic Research Expedition (JARE) and the Australian National Antarctic Research Expedition (ANARE). The orthogonals to the contours are obtained to deduce ice drainage basins.

2. SEASAT Radar Altimetry Data

2.1. *Interim Geophysical Data Record*

SEASAT launched on June 28, 1978, circled the earth with a period of 101 min, an inclination angle of 107.94° and a nominal height of 800 km (TOWNSEND, 1980). Though the SEASAT radar altimeter was designed to measure the topography of oceans, it also acquired ranging of the ice surface of the Antarctic continent. During the sensor operation of 99 days (June 1978–October 1978), SEASAT covered 3×10^6 km^2 of the East Antarctic ice sheet to 72.06°S by more than 450 overflights (ZWALLY *et al.*, 1983).

Figure 2 schematically illustrates range measurements by the SEASAT radar altimeter. Measurement rate of 10 times per second and the groundtrack velocity of 6.62 km/s resulted in a spatial sampling of 662 m apart. The altimeter illuminated 9.5 km

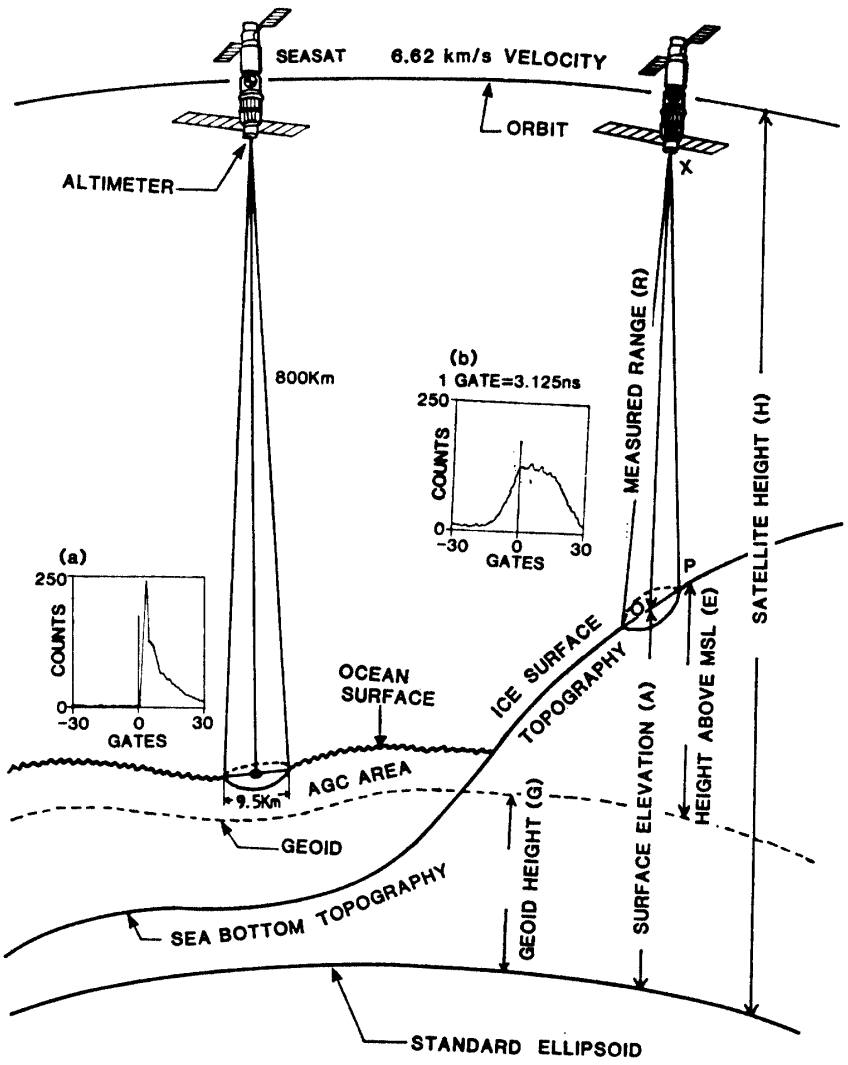

Fig. 2. Schematic illustration of SEASAT altimeter measurement. Height above mean sea level (E) is used for later contouring. As for the explanations of insets (a) and (b), see text.

across the AGC (Auto Gain Control) footprint area, from where radar backscatter contributed to the 60 sample gates with a separation of 3.125 ns (equivalently 46.84 cm) for return-pulse waveform as illustrated in (a) and (b). Over calm oceans, the rise of the return-pulse is very sharp as illustrated in (a). Over sloping or undulating ice surfaces, the return-pulse shape becomes rather broad and indistinct as in (b), showing a complicated nature of the reflection (MARTIN *et al.*, 1983; THOMAS *et al.*, 1983). Since the return-pulse tracking circuit of the altimeter was optimized for use over the oceans of small scale roughness, it is not sufficiently fast to follow the rapidly changing ranges over irregular terrains of Antarctica. The loss of altimetry data usually occurred when the change of altitude was larger than 50 m/s, equivalent to 0.43° in slope inclination. Over gentle slopes, the SEASAT altimeter gives a range (R) with a spatial sampling of every 662 m. Since the satellite position in the earth-centered coordinates is known, satellite height (H) above the WGS-72 Standard Ellipsoid (a=6378135 m,

$f=1/298.26$) can be correlated with (R) at the measuring point. The surface elevation (A) can thus be calculated from (H) minus (R). In order to obtain the distribution of height above mean sea level (m.s.l.) (E), we further subtract the geoid-ellipsoid separation (G) of the GEM10B model (MARSH and CHANG, 1979) from (A). The reduction of (G) from (A) is equivalent to zero-setting the altimeter-derived surface elevations of the Indian Ocean which surrounds the Antarctic sector 0°–90°E.

There are several processing stages of altimetry data such as tropospheric corrections to the measured range and the correction of attitude deflection of the satellite. These corrections are explained in TAPLEY *et al.* (1982). The data used in the present analysis is Interim Geophysical Data Record (IGDR), which was compiled in 1979 by National Aeronautics and Space Administration (NASA), and is the same data used by SEGAWA and ASAOKA (1982) for geoid evaluation around Antarctica. The IGDR can provide the subsatellite ice sheet profile measured above the surface of the WGS-72 Standard Ellipsoid with a sampling time interval of 1-s. This 1-s sampling data is the average of every 0.1-s, and corresponds to spatial sampling of 6.62 km. The precision of the range measured over calm oceans, with the significant wave height lesser than 5.0 m, is estimated to be 0.1 m for 1-s average ranging after the correction for variation in atmospheric path length.

2.2. *Errors in IGDR over the ice sheet*

Imperfect modeling of gravity field and the air drag of the satellite are the main source of errors in orbit determination and the satellite heights at the intersecting point of the two satellite orbits (crossover point) usually differs 5–10 m. In order to adjust inconsistency of orbit height in IGDR, an iterative correction procedure has been applied by SEGAWA and ASAOKA (1982), so that the disagreement in height measurements over the ocean around Antarctica was minimized by the least-squares method. We took their correction values to remove orbit bias error also over the ice sheet and the correction would improve satellite orbit height to 2–3 m accuracy.

Since the ice sheet is sloping, there arizes a "slope-induced error" (BRENNER *et al.*, 1983). Ranges obtained by radar altimetry are distances to the closest point of the surface. Therefore, when the ice sheet is sloping along-track, the reflection point P in Fig. 2 is always lying upslope from the subsatellite point O, causing the slope-induced error between the desired range to the subsatellite point XO and the measured range XP as

$$\Delta R = \mathrm{XO} - \mathrm{XP} = R(1-\cos\alpha) \sim \frac{R\alpha^2}{2},$$

where α is the slope of the surface and R is the satellite orbit height. Substituting $R=$ 800 km and typical value of $\alpha \sim 5\times10^{-3}$ for a plateau area of 2000–3000 m in elevation, the slope-induced error is about 10 m. The slope-induced error attains to 40 m when α is as large as 1×10^{-2} in a coastal area. The correction of slope-induced error becomes further complicated on irregular surface becuase the shortest range is affected by both along- and cross-track slopes.

Since the SEASAT return-pulse tracker is adjusted to the sea surface measurements, the rise of the return-pulse from the ice surface is indistinct as in (b) of Fig. 2, which

introduces uncertainty in determining the returning gate number and requires retracking of the return-pulse waveform. MARTIN *et al.* (1983) estimate a typical range error of 14 m in the case without retracking.

During IGDR processing, the above-mentioned errors should be taken into account and these errors may be coupling each other to give unpredicted errors in height above m.s.l. (E). In a coastal area where the altitude is less than 500 m, the height error may reach up to 100–150 m. Even in a plateau area, the height error might sometimes attain to 50 m. Thus, the 100 m contouring was decided for the area higher than 500 m.

3. Ice Sheet Configulation

Figure 3 illustrates superposition of IGDR along 85 subsatellite groundtracks over the region north of 72°S from 0° to 90°E. This pass coverage helps computer contouring of the area between 30° and 80°E, where a comparatively large number of ground survey data are distributed. The blank portion in each groundtrack of Fig. 3 corresponds to the loss of altimetry data as described in Section 2. The groundtracks become dense near 72.06°S with 1.0 km spacing, whereas they are sparse in the coastal region with a horizontal spacing of 100 km.

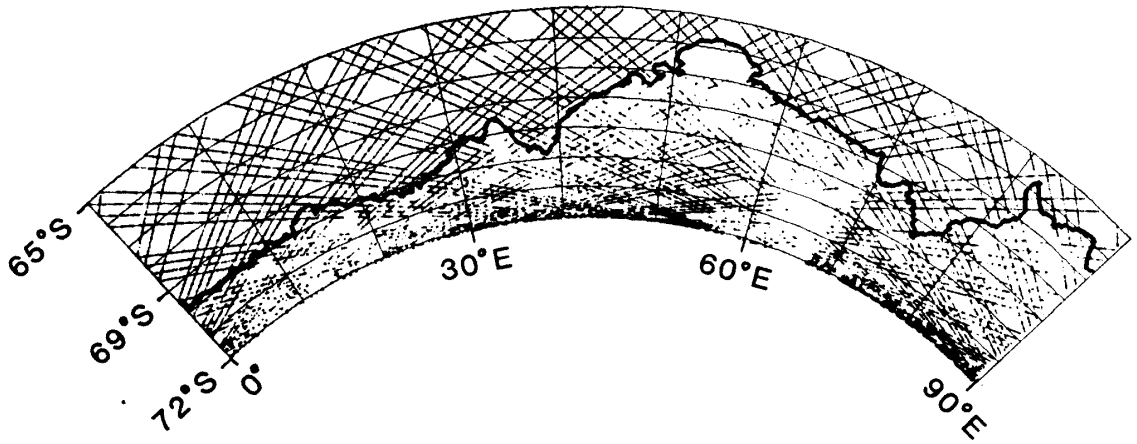

Fig. 3. Superposition of 85 subsatellite groundtracks over the sector 0°–90°E. Blank portions indicate loss of altimetry data.

Figure 4a illustrates an example of calculated surface elevation above m.s.l. along the groundtrack No. 492 (Fig. 4b) from point A (70.00°S, 55.82°E) to point B (70.44°S, 3.10°E). The surface elevation decreases with an overall declination of 1.3×10^{-3} along the subsatellite track, showing a large undulation with the wave-length of 400–700 km. The enlarged portion between points C (71.35°S, 44.81°E) and D (72.06°S, 28.42°E) (Fig. 4c) shows an ice-covered rise in the southeastern part of the Yamato Mountains. It is to be seen that the rise has the height of 350 m within the distance of 200 km, suggesting the existence of a subglacial bedrock rise which may continue to the Riiser-Larsen Peninsula (Fig. 1). Another rise in the lower portion of Fig. 4a corresponds to the Sør Rondane Mountains. Because of outcrop areas and rapidly changing surface

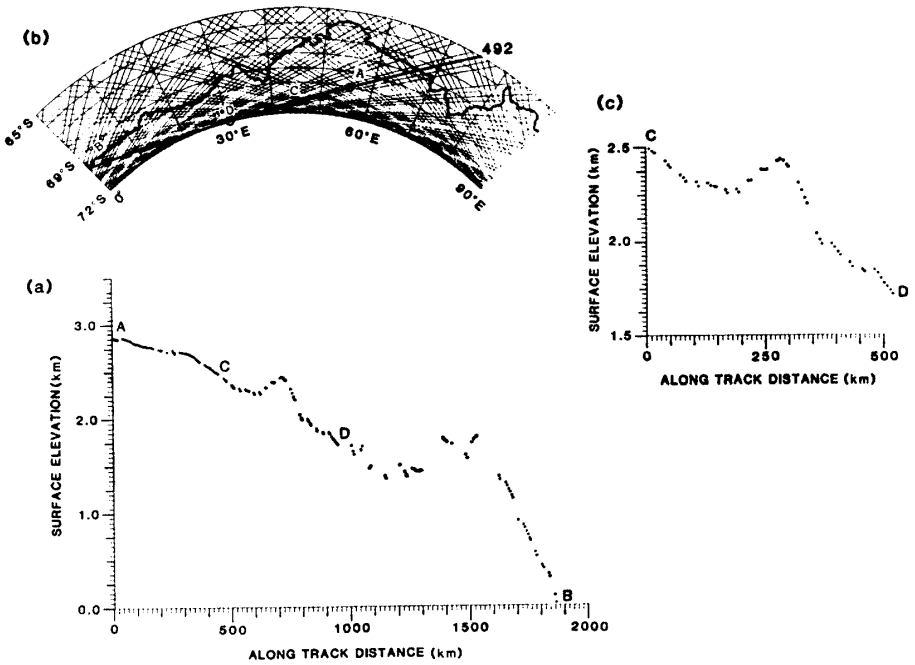

Fig. 4. (a) Surface elevation along subsatellite groundtrack No. 492. (b) No. 492 passes from west of the Lambert Glacier through Mizuho Plateau and the Yamato Mountains to the Sør Rondane Mountains. (c) Enlarged portion of the rise between points C and D of the ice-covered area in the southeast of the Yamato Mountains.

undulations, the loss of altimetry data occurred frequently.

Using a total of 7480 data points of 6.62 km spacing in the sector 30°–80°E, computer contouring is made by gridding the area into rectangles with side lengths of 0.1° in latitude (11.1 km) and 0.4° in longitude (13.8–18.8 km, depending on latitude). All the elevations measured within a rectangle (or from neighboring points when there is no altitude data in the rectangle) are averaged with the assigned weights which are inversely proportional to the distances from the grid point.

Figure 5 illustrates the obtained map of the ice sheet in the sector 30°–80°E. Since there are less elevation data in the Napier Mountains and Lambert Glacier areas as shown from Figs. 1 and 3, the contours in these areas are illustrated by broken curves, because it was foreseen that there may be erroneous deformation in the computer-aided contouring. Figure 6 illustrates three-dimensional display of Fig. 5 which is viewed from the Indian Ocean; it clearly shows east-west breakup of the ice sheet by the Lambert Glacier and the Amery Ice Shelf.

The characteristic configuration features deduced from Figs. 5 and 6 (hereafter denoted as the SEASAT configuration) are: (a) There is a ridge which starts from (72°S, 52°E) and the ridge has a gentle declination of $5.0–7.0 \times 10^{-4}$ to NE. (b) The surface slope values increase with lowering elevation near the coast. The steepest slope of about 1.1×10^{-2} exists around (70°S, 39°E) at the mouth of Shirase Glacier. This steep inclination may be related with the fast-flowing Shirase Glacier where NAKAWO *et al.* (1978) measured its velocity as 2500 m/a. (c) In spite of sparse footprint data in the

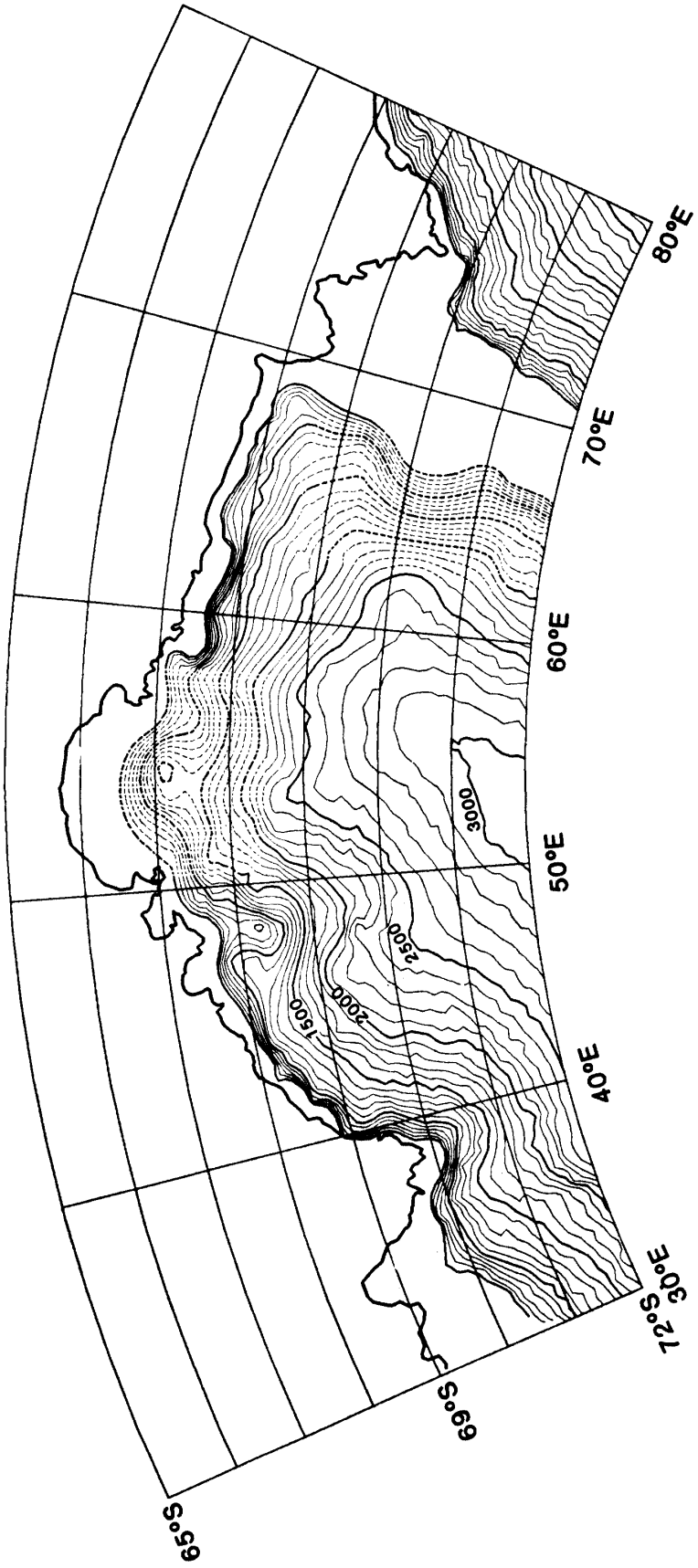

Fig. 5. The 100 m contouring by the SEASAT altimetry data in the sector 30°–80° E. Broken portions correspond to uncertain contouring by sparse footprint data.

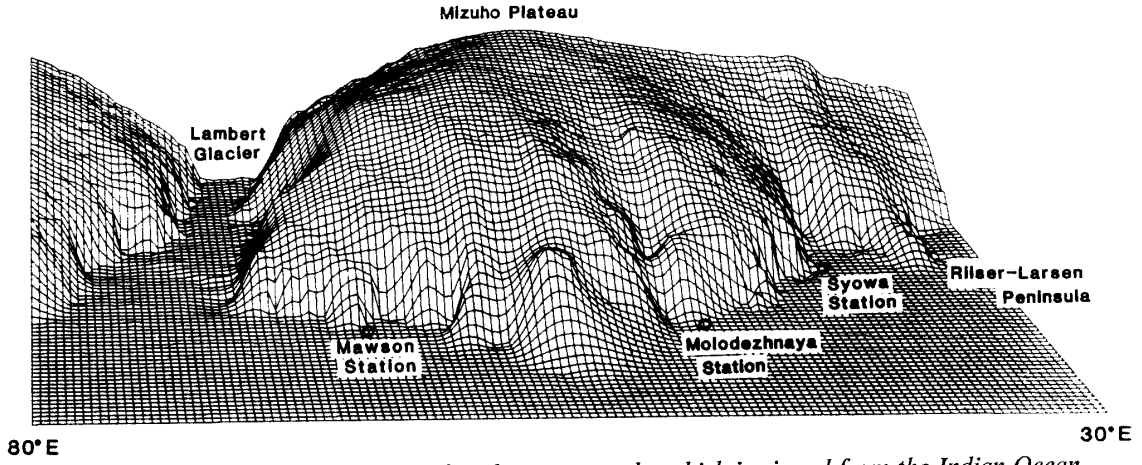

Fig. 6. Three-dimensional display of surface topography which is viewed from the Indian Ocean.

coastal region, the SEASAT configuration shows mounds at (67°S, 54°E) and (68°S, 48°E). They rather faithfully reflect the topography of the Napier Mountains and the Nye Mountains, respectively when compared with the SPRI map (Fig. 1). (d) The SEASAT configuration has a 3000-m contour which reaches 71°S. The trough around 55°E in the SEASAT configuration is not so clear as in the case of the SPRI map.

The SPRI map on a scale of 1 : 6000000 is compiled from the data of airborne radio-echo sounding altimetry, TWERLE (Tropical Wind Energy Conversion and Reference Level Experiment) altimetry by LEVANON *et al.* (1977), oversnow barometric altimetry, geodetic leveling, satellite Doppler determined elevation and SEASAT radar altimetry (DREWRY, 1983). However, corrections of orbital-bias-error for SEASAT altimetry data are not included in the SPRI map. Satellite Doppler stations occupied by JARE were installed after 1980 and the results were not included in the SPRI map. The configuration map in Fig. 5 is compiled only from SEASAT altimetry data and the overall accuracy is to be estimated by comparing with the ground survey data obtained by JARE and ANARE.

4. Comparison with Ground Survey Data

Figure 7 shows distribution of ground survey data in the sector of 30°–80°E. Along Route A running approximately along 72°S, NARUSE (1978) made triangulation survey in November 1973 and obtained 164 elevation data above m.s.l. with an accuracy less than 0.1 m. In order to estimate the elevation of Route A in June 1978 when the SEASAT data was available, the change of elevation in 4.5 years has to be estimated. Along Route A, the ice surface is lowering with the velocity of around $0 \sim -1.0$ m/a (NARUSE, 1978). Together with reasonably assumed ablation of 0–0.1 m/a, the surface declination is -2×10^{-3} and the surface flow velocity is 0–20 m/a (NARUSE, 1978), thus the decrease in elevation is estimated to be 2.0–5.0 m depending on locations. After considering the decrease of surface elevation and transforming the station coordinates from the Bessel Reference Ellipsoid to the WGS-72 Standard Ellipsoid, comparison of triangulation elevation data at a spatial interval of 7–10 km with the corresponding SEASAT elevation data was made (open circles in Fig. 7). In Table 1a or 1b, height difference is defined

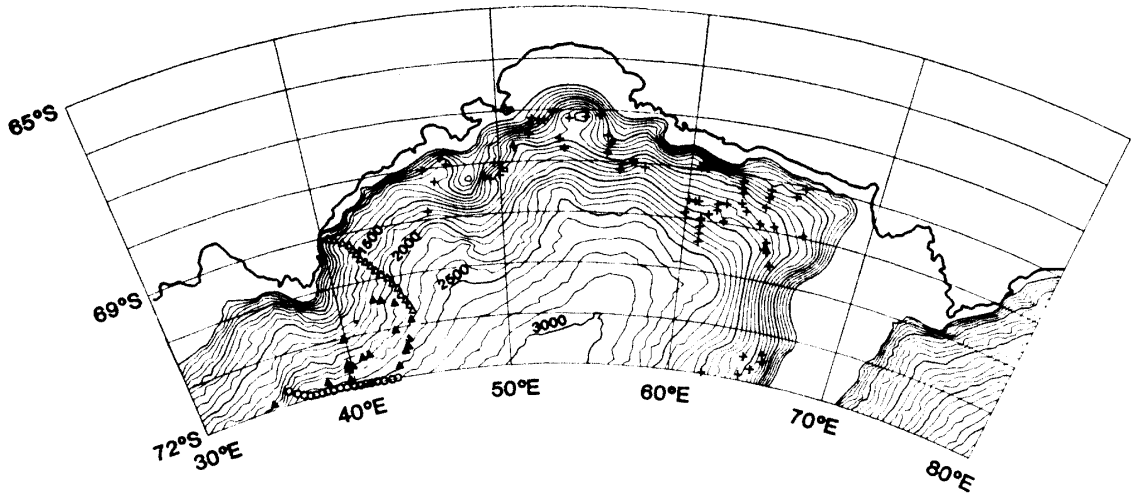

Fig. 7. Distribution of ground data for comparison with the SEASAT elevation. Open circles are from triangulation survey in 1973. Open triangles are obtained by satellite Doppler positioning in 1980, while solid triangles are obtained in 1982, 1983 and 1984. Crosses indicate data picked from 1 : 1000000 Topographic Map 25/09/18.

by SEASAT elevation minus ground survey height. The SEASAT elevation is on an average 0.5 m lower than the triangulation elevation as given in the first raw of Table 1a.

A total of 50 satellite Doppler stations are taken by JARE in the elevation range of 500–3000 m in the sector of 30°–80°E. Open triangles in Fig. 7 indicate satellite Doppler stations along Route S–H–Z taken in November 1980 (SHIBUYA and ITO, 1983). Since the obtained antenna height is the elevation above the WGS-72 Standard Ellipsoid, it is reduced to the elevation above m.s.l. by correcting the geoidal undulations of the GEM10B model coefficients. The ground height data are further corrected for snow ablation/accumulation and the effect of ice sheet flow during 1978–1980. Solid triangles indicate similar satellite Doppler stations obtained in 1982 (NISHIO *et al.*, 1986), in 1983 (NAKAWO *et al.*, 1984) and in 1984 (FUJII *et al.*, 1986). The SEASAT elevation is compared with the ground height without correcting height change because there is no available data yet for these stations.

Crosses indicate elevations above m.s.l. by ANARE which are taken from the 1: 1000000 "Topographic Sheet of Molodezhnaya-Mawson" published by the Department of National Development and Energy (Map 25/09/18). A total of 77 ground data in the map are compared with the SEASAT elevations.

Since errors in the SEASAT elevation are different in elevation, the height difference is summarized into 5 elevation ranges as shown in Table 1a according to the survey method. The average of the height difference is mostly within −10 to 10 m except the elevation range of 500–1000 m. As for the standard deviation, there is little difference among satellite Doppler positioning, triangulation survey and Topographic Map 25/09/18 and the value ranges from ±10 m to ±30 m. Table 1a may thus be re-summarized as Table 1b. A total of 157 ground data give an overall accuracy of 2.2 m average height difference with the standard deviation of ±21.5 m. As compared with ±2 m standard deviation of BROOKS *et al.* (1978) or ZWALLY *et al.* (1983), the resultant standard deviation in the present study is greater by one order of magnitude.

Table 1a. Comparison of SEASAT elevation with ground data.

Elevation range (m)	Method	Number of data point	Height difference* mean (m)	Height difference standard deviation (m)
2000–3000	Satellite Doppler positioning[1)]	31	6.8	±17.5
	Triangulation survey[2)]	30	−0.5	±10.4
	Topographic Map 25/09/18[3)]	7	9.4	±24.4
1500–2000	Satellite Doppler positioning	11	9.2	±21.9
	Topographic Map 25/09/18	29	−4.0	±23.3
1000–1500	Satellite Doppler positioning	7	3.0	± 7.7
	Topographic Map 25/09/18	32	−1.9	±28.3
500–1000	Satellite Doppler positioning	1	27.8	
	Topographic Map 25/09/18	9	12.3	±26.9

* Height difference is defined by SEASAT elevation minus ground height.
1) Measured in 1980, 1982, 1983 and 1984 using JMR-1 or JMR-4A two-wave NNSS receiver.
2) Measured in 1973 along Route A running approximately parallel along 72°S.
3) Molodezhnaya-Mawson 1 : 1000000 sheet published by the Department of National Development and Energy, Australia.

Table 1b. Summary of comparison of SEASAT elevation with ground data.

Elevation range (m)	Number of data point	Height difference* mean (m)	Height difference standard deviation (m)
2000–3000	68	3.8	±15.9
1500–2000	40	−0.4	±23.4
1000–1500	39	−1.0	±25.8
500–1000	10	13.9	±25.8
500–3000 (whole range)	157	2.2	±21.5

* Defined same as Table 1a.

There are three factors in large standard deviation of height difference. On the ice sheet of the sector 30°–80°E, satellite orbital heights still have ±6.7 m standard deviation at the 147 crossover points. SEASAT ranging without retracking and imperfect modeling of GEM10B geoid over Antarctica result in further uncertainty of calculated surface elevation above sea level. The height change in the time interval between the SEASAT altimetry in 1978 and the ground survey in 1973–1986 may be too large to be accurately estimated or may depend on small-scale locality.

5. Ice Divides and Concluding Remarks

Using the digital elevation data which gave Fig. 5, computer tracing of orthogonals to the elevation contours is made. The area of Fig. 5 was divided into rectangle grids (0.1° latitude by 0.2° longitude) and a cubic-surface-fitting for the rectangle elements around the grid point is made. The derivatives of height with respect to latitudinal and

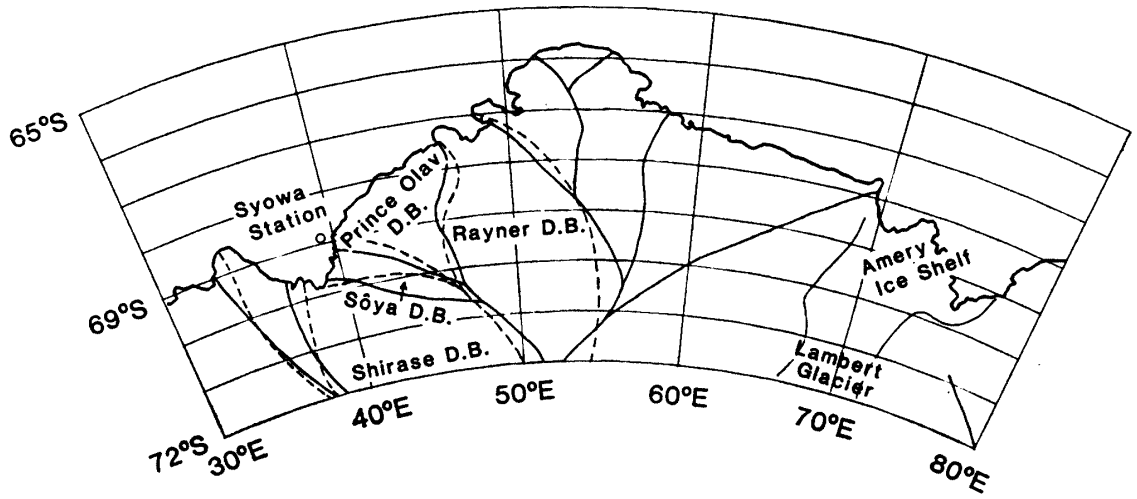

Fig. 8. Ice divides obtained from computer tracing of the orthogonal directions to the equal elevation contours in Fig. 5 (solid curves) and those by the oversnow ground survey (broken curves). The names of the drainage basins are after SHIMIZU *et al. (1978).*

longitudinal directions were calculated at the grid point. By windowing and shifting the number of rectangle elements, the most appropriate direction of the maximum slope for the fitted-surface was searched and traced to obtain the ridge lines as indicated by solid curves in Fig. 8.

As compared with the previously estimated ice divides (broken curves in Fig. 8) from the oversnow traverse surveys (SHIMIZU *et al.*, 1978), the ice divides derived from the SEASAT altimetry data show a slight change of the ice drainage basins. The eastern boundary of the Rayner drainage basin at 70°30'S extends further east but shifts to west at 72°S, narrowing the previously obtained drainage basin at higher latitude. The boundaries of the Sôya drainage basin shift toward south and broaden the previously obtained drainage area. It is noted that the Lambert Glacier has a vast drainage basin extending from 53° to 80°E.

The satellite altimetry yields numerous ice sheet elevation data within 2–3 months. When the accuracy of configuration map is improved less than 1 m by increasing the footprint density and ground data, repeated satellite mapping of the ice sheet surface elevation at intervals of 5–10 years would provide very accurate information on Antarctic glaciology.

Acknowledgments

The authors express their sincere thanks to Dr. T. MATSUMOTO and Ms. K. TAKAHASHI of the Ocean Research Institute, University of Tokyo for their help in computer processing. Prof. M. SAITO of Kobe University kindly provided the computer program of calculating maximum regional slope vectors. Information from Dr. BROOKS and Dr. ZWALLY was stimulative for our study. SEASAT IGDR was provided for the authors through Remote Sensing Technology Center of Japan. Calculations were made by HITAC M-180 at the National Institute of Polar Research.

References

BRENNER, A. C., BINDSCHADLER, R. A., THOMAS, R. H. and ZWALLY, H. J. (1983): Slope-induced errors in radar altimetry over continental ice sheets. J. Geophys. Res., **88**, 1617–1623.

BROOKS, R. L., STANLEY, H. R., CAMPBELL, W. J., ZWALLY, H. J. and RAMSEIER, R. O. (1978): Ice sheet topography by satellite altimetry. Nature, **274**, 539–543.

DREWRY, D. J., ed. (1983): The surface of the Antarctic ice sheet. Antarctica; Glaciological and Geophysical Folio. Cambridge, Scott Polar Res. Inst., sheet 2.

FUJII, Y., KAWADA, K., YOSHIDA, M. and MATSUMOTO, S. (1986): Glaciological Research Program in East Queen Maud Land, East Antarctica, Part 4, 1984. JARE Data Rep., **116** (Glaciol. 13), 71 p.

LEVANON, N., JULIAN, P. R. and SUOMI, V. E. (1977): Antarctic topography from balloons. Nature, **268**, 514–516.

MARSH, J. G. and CHANG, E. S. (1979): Global detailed gravimetric geoid. Mar. Geod., **2**, 145–159.

MARTIN, T. V., ZWALLY, H. J., BRENNER, A. C. and BINDSCHADLER, R. A. (1983): Analysis and retracking of continental ice sheet radar altimeter waveforms. J. Geophys. Res., **88**, 1608–1616.

NAKAWO, M., AGETA, Y. and YOSHIMURA, A. (1978): Discharge of ice across the Sôya Coast. Mem. Natl Inst. Polar Res., Spec. Issue, **7**, 235–244.

NAKAWO, M., NARITA, H. and ISOBE, T. (1984): Glaciological Research Program in East Queen Maud Land, East Antarctica. Part 2, 1983. JARE Data Rep., **96** (Glaciol. 11), 80 p.

NARUSE, R. (1978): Studies on the ice sheet flow and local mass budget in Mizuho Plateau, Antarctica. Contrib. Inst. Low Temp. Sci., Hokkaido Univ., Ser. A, **28**, 1–54.

NISHIO, F., OHMAE, H. and ISHIKAWA, M. (1986): Glaciological research program in East Queen Maud Land, East Antarctica, Part 3, 1982. JARE Data Rep., **110** (Glaciol. 12), 37 p.

SEGAWA, J. and ASAOKA, T. (1982): Reevaluation of Geoid based on the SEASAT altimeter data —Geoid around Antarctica—. J. Geod. Soc. Jpn., **28**, 162–171.

SHIBUYA, K. and ITO, K. (1983): On the flow velocity of the ice sheet along the traverse route from Syowa to Mizuho Stations, East Antarctica. Mem. Natl Inst. Polar Res., Spec. Issue, **28**, 260–276.

SHIMIZU, H., YOSHIMURA, A., NARUSE, R. and YOKOYAMA, K. (1978): Morphological feature of the ice sheet in Mizuho Plateau. Mem. Natl Inst. Polar Res., Spec. Issue, **7**, 14–25.

SOVETSKAYA ANTARKTICHESKAYA EKSPEDITSIYA (1966): Obschegeograficheskie karty, Antarktika 1: 20000000 (General maps, Antarctica 1 : 20000000). Atlas Antarktiki 1 (Atlas of Antarctica 1). Moskva, Gravnoe Upravlenie Geodezii i Kartografii, 16–17.

TAPLEY, B. D., BORN, G. H. and PARKE, M. E. (1982): The SEASAT altimeter data and its accuracy assessment. J. Geophys. Res., **87**, 3179–3188.

THOMAS, R. H., MARTIN, T. V. and ZWALLY, H. J. (1983): Mapping ice-sheet margins from radar altimetry data. Ann. Glaciol., **4**, 283–288.

TOWNSEND, W. F. (1980): An initial assessment of the performance achieved by the SEASAT-1 radar altimeter. IEEE J. Oceanic Eng., **5**(2), 80–92.

ZWALLY, H. J., BINDSCHADLER, R. A., BRENNER, A. C., MARTIN, T. V. and THOMAS, R. H. (1983): Surface elevation contours of Greenland and Antarctic ice sheets. J. Geophys. Res., **88**, 1589–1596.

(Received March 24, 1986; Revised manuscript received June 24, 1986)